Assiut Univ. J. of Physics **Printed ISSN 1687-4900**
48(2), pp.45-69 (2019)

SYNTHESIS AND CHARACTERIZATION OF REDUCED GRAPHENE OXIDE/ZINC OXIDE NANOCOMPOSITES

A. A. Ebnalwaled[1], A. Abu El-Fadl[2,*], Muhammad A.Tuhamy[2]
[1] South Valley University, Faculty of Science, Department of Physics, Qena 83523, Egypt
[2]Assiut University, Faculty of Science, Department of Physics, Assiut 71516, Egypt
E-mail: abulfadla@yahoo.com

Received: 18/8/2019 **Accepted:** 2/9/2019 **Available Online:** 1/12/2019

Reduced graphene oxide/zinc oxide (RGO/ZnO) nanocomposites were synthesized by facile hydrothermal method; this method consists of exfoliation of graphite with modified Hummer's method and synthesis of (RGO/ZnO) nanocomposites using hydrothermal method. X-ray diffraction, TEM and FT-IR spectroscopy were used for structure morphological characterization. Optical properties of the samples were studied by measuring their optical-absorbance. It can be concluded from XRD analysis that there are improvements of crystallinity associated with the increase of the crystallite size, as well as the increase in both of the (Zn-O) bond length and unit cell volume with the increase of ZnO ratio in RGO/ZnO nanocomposites. The morphological studies confirmed that the scale of ZnO particles is large and the size distribution is not uniform in samples of RGO/ZnO and that most particles have average size of about 9 nm while some particles even have larger size. The optical absorption spectra show that the excitonic peak of the as-prepared samples is red shifted from 268 nm to 376 nm for reduced grapheme oxide (RGO) with the increase of ZnO ratio, and the optical band gap changes from 2.39 for pure RGO to 3.34 eV for pure ZnO. The effect of UV irradiation on the optical absorption nanocomposites at different UV doses was carried out using UV lamp.

1. INTRODUCTION

ZnO nanomaterials are attractive candidates for fabricating biosensors, super capacitors, solar cells, and another several electronic devices because of their diverse range of nanostructures, high electron mobility, chemical stability, and electrochemical activity, high isoelectric points which promote enzyme adsorption, bio compatibility, and piezoelectric properties [1]. Graphene which is a new important member in the family of carbon can be described as mono layer or a few layers of 2D planar sheet of sp^2 hybridized

carbon atoms arranged in a hexagonal lattice was first synthesized by modified Hummer's method [2]–[4]. It is a very good choice for electrode because of its characteristics, like excellent electrical conductivity, fast electron mobility, high surface area to volume ratio, and very good thermal and electrochemical properties [5]. Graphene has been widely studied for use in many electronics applications, due to its large theoretical surface area, good electronic conductivity, mechanical properties, and exceptional thermal stability, high electrical activity, good optical transmittance [6]. Graphene as a new member of the family of carbon can be used as an ideal choice for preparing nanocomposites like metal oxides, metal sulfides and metal nanoparticles for improved properties. The graphene based materials are widely used in several applications like, photo catalysis [7], energy storage, gas sensors [3]and biosensors [3], [8]–[12], light emitting diodes (LED) [13] Graphene and other carbon-based materials show a good conductivity when they coupled with metal oxides [14].

Reduced Graphene oxide has been synthesized by different methods such as chemical vapor deposition (CVD), micro mechanical exfoliation, epitaxial growth, thermal reduction and chemical methods (modified Hummer method) [2], [15]. Among those methods Hummer's method and it's modifies are the most used methods [16].

Among the many metal oxides, zinc oxide (ZnO) is the most attractive as a promising material because of its low cost, rich availability, environmental friendly nature and electrochemical activity and direct wide band-gap about 3.37 eV [1]. RGO/ZnO nanocomposites may exhibit unique properties due to the interactive effect between graphene and ZnO for improved electrical conductivity and electron transfer rate (electron mobility) [17]. The attracting properties of graphene/ZnO nanocomposites have been widely studied like enhanced photo catalytic performance [18], energy storage capability, sensing property, optoelectronic property and ultra-fast nonlinear optical switching ability [19].

In the present investigation reduced graphene oxide synthesized by modified Hummer's method, Zinc oxide synthesized by hydrothermal method, and RGO/ZnO nanocomposites were synthesized by hydrothermal method and various characterization techniques have been employed to investigate the structure morphology and optical absorption and of the prepared samples.

2. Experimental

2.1. Materials

Graphite powder (99%) and hydrazine hydrates purchased from Fisher Scientific, (United Kingdom), zinc acetate dihydrate ($(CH_3COO)_2\ Zn_2.H_2O$) (98%) purchased from Oxford Laboratory Reagent, India, sodium hydroxide pellets (NaOH) purchased from Fisher Scientific, United Kingdom, potassium permanganate ($KMnO_4$) (99%), sulfuric acid (98%), hydrochloric acid (HCl) (38%) and hydrogen peroxide (H_2O_2) (30%) purchased from El Nasr Pharmaceutical Chemical Egypt. All the commercial chemical reagents which used in this experiment were used without further precipitation and distilled water was used in all experiment.

ZnO nanoparticles were prepared according to equations (1), (2) and the residual sodium salt CH_3COONa was removed by washing the sample with absolute ethanol and distilled water for several times [15], [16], [19].

$$Zn(CH_3COO)_2.2H_2O + 2NaOH \rightarrow Zn(OH)_2 + 2CH_3COONa + 2H_2O \quad (1)$$

$$Zn(OH)_2 + 2H_2O \rightarrow Zn(OH)_4^{-2} + 2H^+$$

$$Zn(OH)_4^{-2} \rightarrow ZnO + H_2O + 2OH \quad (2)$$

2.2. Preparation of reduced graphene oxide (RGO)

Reduced graphene oxide in nano form prepared via modified Hummer's method. Reduced graphene oxide (RGO) synthesis can be distinguished into two major steps, firstly oxidation of graphite flakes into exfoliated graphene oxide (GO) and reduction GO into RGO, starting with graphite powder washed with hydrochloric acid (HCl) then washed with distilled water several times, then the powder dissolved in concentrated sulfuric acid. Soft potassium permanganate added wisely to the solution, the solution temperature must be less than 20 °C by putting the mixture in ice bath. After stirring for 45 minutes the mixture diluted by adding wisely 100 ml of distilled water. The mixture heated up to 90 °C then 40 ml of hydrogen peroxide added, after stirring for 30 minutes the mixture let a night to precipitate and washed by HCl then washed several times by distilled water and then the powder was filtered and graphite oxide powder was obtained [3], [4], [16], [20]. Graphite oxide powder was dissolved in distilled water and the black suspension transferred into sonication (50 Hz) for 180 min at room temperature to exfoliate the stacked graphite oxide sheets into graphene oxide (GO), then the black suspension centrifuged for 30 min at 1000 rpm to remove the aggregation from graphene oxide also to remove the unexfoliated graphite, then the powder was filtered and washed by distilled water and

ethanol several times, and dried at 100 °C. The second step to obtain reduced graphene oxide is reducing the obtained graphene oxide by adding 0.5 g of the obtained GO to 1000 mL of distilled water and 5mL of hydrazine hydrate then the mixture transferred into reflux system at 100 ºC for 24 h. to reduce graphene oxide into reduced graphene oxide (removing oxygen containing groups). For 24 hours then suspension washed several times by distilled water then filtered and dried at 100 to obtain RGO.

2.3. Preparation of reduced graphene oxide (RGO) /zinc oxide (ZnO) nanocomposites.

Reduced graphene oxide (RGO) powder and zinc acetate in different ratios as shown in table 1 are dissolved in water and stirred for 15 min, then 1M of NaOH dropped wisely to the mixture until achieve pH= 10 and the white mixture was transferred into Teflon autoclave hydrothermal system for 24 h at 100 °C, then the product powder was filtered and washed by distilled water and ethanol, then dry at 100 °C.

Table1. Different mass ratios of reduced graphene oxide to zinc oxide precursor used to form RGO/ZnO nanocomposites.

Name of sample	Mass of RGO (g)	Mass of zinc acetate (g)	Weight ratio of graphene: zinc
ZnO	0	5	ZnO
RGO	1	0	RGO
G/Zn 1	1	1	1:1
G/Zn 2	1	2	1:2
G/Zn 3	1	3	1:3
G/Zn 4	1	4	1:4
G/Zn 5	1	5	1:5

2.4. Instrumentation and characterizations

The phase and crystal size of the prepared samples were characterized using an automated X-ray powder diffractometer (Philips diffractometer 1710 with Cu target and graphite monochrometer with the incident wavelength of 0.15418 nm). The morphological studies of samples were carried out using a

transmission electron microscope (TEM) [JEOL JEM 1010] Japan performed at acceleration voltage of 200 KV]. Fourier transform infrared spectroscopy (FT-IR) analysis was carried out on a (Jasco Model-4000 Japan) 360 spectrometer to determine the specific functional groups present on the surface by KBr method. UV-VIS spectrophotometer, UV2300, TECNOMOP was used to measure the absorbance, and transmittance of the prepared sample with wavelength scan from 190 to 1100 nm.

UV effect on the optical absorption at different exposure time (t) with the same concentration of collcial solution were studied using mercury lamp model power of 6 watt, UV irradiation wavelength λ=254 nm) and flux intensity of 6.9 mW/cm^2

3. RESULTS AND DISCUSSION

3.1. Structural studies

The crystalline structures, crystal size and phase purity of RGO, zinc oxide powder, and RGO/ZnO nanocomposites in different ratios were studied using XRD. The XRD patterns of the as synthesized pure ZnO and Pure RGO are shown in Fig. 1. (a) The XRD patterns of the synthesized (RGO/ZnO) nanocomposites materials are shown in Fig. 1. (b) XRD patterns were calculated in the range of 20◦ to 80◦ with step 0.06◦. XRD main peaks are shown in Fig. 1. (a) indicate the presence of highly crystalline ZnO nanoparticles with a hexagonal structure (ICDD card no: 00-001-1136) with calculated d-spacing of 2.7 Å and a=b=2.5Å and c=3.99Å. Zinc oxide main peaks are sharp and confirming high crystallinity of the samples with main peak at2Θ=36.52^o (101). These peaks correspond to (100), (002), (101), (102), (110), (103), (200), (112), and (201) crystalline planes related to the standard data of the ZnO. It is observed that peaks corresponding ZnO crystalline phase were detected in the XRD patterns of the samples with 2Θ values (31.977, 34.64◦, 36.52◦, 47.77◦, 56.833◦, 63.096◦, 66.607◦, 68.181◦, 69.31◦, 72.804◦, 77.182◦, 81.52◦, 89.823◦) with hexagonal structure. Although in Graphene Main peaks are existed at 2Θ=26.324◦, 42.28◦, 44.32◦, 54.411◦, and 72.16^o with hexagonal structure (ICDD card no: 00-001-0640) corresponding to d-spacing of 2.799 Å, a=b= 3.506Å and c=5.598Å.

Fig. 1. (b) show that Zinc oxide main characterizing peaks appear with small intensity at RGO/Zn1 then the peaks intensity increase directly through different weight ratios from RGO/Zn1 to RGO/Zn5 although the intensity of graphene characterizing main peak with decreased. Fig. 2. show the graphene

main characterizing peak in different composite ratios was shifted to right with the increasing of zinc oxide continent in the composite. The strong and sharp zinc oxide characterizing peaks in RGO/ZnO nanocomposites tell us that the ZnO nanoparticles stacked to graphene nanosheets are still crystalline as in the pure sample.

The lattice constants a, and c of a hexagonal plane for ZnO, RGO and RGO/ZnO nanocomposites are calculated using the following equation:

$$\frac{1}{d^2} = \frac{4}{3}\left(\frac{h^2+hk+k^2}{a^2}\right) + \frac{l^2}{c^2} \quad (3)$$

For hexagonal crystal system the unit cell volume can be calculated using the equation:

$$V=0.866\ a^2c$$

In the other hand the bond length (L) can be evaluated by the equation:

$$l = \sqrt{\frac{a^2}{3} + (\frac{1}{2} - z)^2 c^2} \quad (4)$$

Where $z = \frac{a^2}{3} + \frac{1}{4}$ (5)

The average particle sizes can be estimated from peak by using Debye–Scherrer's formula according to the following equation [21]:

$$D_{hkl} = \frac{0.94\lambda}{\beta_{hkl}\cos\theta} \quad (6)$$

Where λ is the wavelength of the incident X-ray beams (λ= 1.5418 Å), θ is the diffraction angle, and β_{hkl} is the FWHM corrected for the instrumental broadening of the XRD peaks. It is found that the grain size of the samples are start with RGO about 8.8 nm in graphene and increases with increase of zinc oxide ratio in nanocomposites to reach about 22.5 nm in RGO/Zn5 and reaches 24.8 nm for pure ZnO sample. These findings indicate that the ZnO decorated on the RGO nanosheets in RGO/ZnO nanocomposites with a particle size ranges from 8.8 to 24.8 nm (according to the Debye–Scherer's formula). The increasing in grain size due to the increase in the both of Zn-O bond length and unit cell volume with increase in ZnO mass ratio.

Crystallite size and lattice strain is determined using Williamson-Hall (W-H) equation [22]:

$$\frac{\beta\cos\theta}{\lambda} = \frac{1}{D} + \frac{4\varepsilon\sin\theta}{\lambda} \quad (7)$$

Where β is the full width at half maximum (FWHM), Θ is the diffraction angle, λ is X-ray wavelength, D is the crystalline size and ε is the lattice strain.

The dislocation density (δ) was calculated using the relation [23]:

$$\delta = 1/D^2 \quad (8)$$

According to Hook's law, for small dislocations in a lattice, a linear relation between the stress σ and strain is given as $\sigma = Y\varepsilon$, where Young's modulus Y (for hexagonal structure) can be represented by the following relation:

$$\mathbf{Y} = \frac{\left(h^2+\frac{(h+2k)^2}{3}+\left(\frac{al}{c}\right)^2\right)^2}{s_{11}\left(h^2+\frac{(h+2k)^2}{3}\right)+ s_{33}\left(\frac{al}{c}\right)^4 + (2s_{13}+ s_{44})\left(h^2+\frac{(h+2k)^2}{3}\right)\left(\frac{al}{c}\right)^2} \quad (9)$$

Where s_{11}, s_{13}, s_{33} and, s_{44} are the lattice compliances of ZnO which equal to $7.858\text{x}10^{-12}$, $-2.206\text{x}10^{-12}$, $6.940\text{x}10^{-12}$, and $23.57\text{x}10^{-12}$ m^2N^{-1} respectively. The energy density u (the energy per unit volume of a lattice) can be calculated from Hook's law $u = (\varepsilon^2 Y_{hkl})/2$. Values of ε, Y, σ, u, and the above-mentioned parameters of all samples are listed in table (2).

Table 2 The diffraction angle (2θ) value, crystallite size (D), lattice parameters (a, c and c/a), unit cell volume (V), internal local strain (ε), dislocation density (δ), Young modulus (Y), internal stress (σ), and energy density (u) for Reduced graphene oxide/zinc oxide (RGO/ZnO) nanocomposites (main peak).

Name of the sample	2 Θ in main peak	D_{hkl} (nm)	Lattice parameter			V ($Å^3$)	ε x10^{-4} radians	□x10^{15} l/m^2	Yx10^{11} (Pascal)	σx10^8 (Pascal)	ux10^5 (J/m^3)
			a (Å)	c (Å)	c/a						
ZnO	36.52	24.8	3.621	5. 78	1.596	65.6	14.6	1.62	2.47	3.6	5.26
RGO	26.324◦	8.8	3.192	5.103	1.596	44.9	75.9	12.9	2.36	17.9	135.1
G/Zn 1	26.551	17.7	3.384	5.402	1.596	53.5	24.8	4.6	1.76	4.36	10.8
G/Zn 2	26.541	17.3	3.465	5.432	1.596	57.5	20.9	3.31	1.83	2.89	8,38
G/Zn 3	26.63	17.46	3.459	5.422	1.596	57.8	20.8	3.2	1.83	2.84	7.95

G/Zn 4	26.48	18.5	3.469	5.538	1.596	57.7	20.1	2.9	1.84	2,68	5.68
G/Zn 5	26. 43	22.5	3.566	5.693	1.596	62.69	16.3	1.9	1.84	2.41	3.9

The crystallite size D_{hkl} corresponds to main peak 2 Θ =26.324◦ (002) in graphene and 2 Θ=36.52(101) in ZnO (other values recorded in table 2) was estimated using the Debye–Scherrer's formula.

3.2. Morphological Studies

The TEM results manifest the transparent nature of the reduced graphene oxide indicating graphite was exfoliated into thin planar sheets and deposition of ZnO nanoparticles on the surface of the RGO sheets, which agree with the XRD pattern. Fig. 4. (a,b) show TEM image with magnification =100000x. It is clear to find that the scale of the ZnO particles is large (compared with RGO nanosheets) and the size distribution is not uniform in sample of RGO/ZnO and that most particles have average size of about 24 nm while some particles even have larger size and others has a smaller size. It is known that HRTEM uses both the transmitted and the scattered beams to create the image. As shown from Fig. 4. (a, b) the uniform size and shape distribution of ZnO obtained at low hydrothermal reaction time and temperature have semi-spherical shape. From the HRTEM the nano size of the obtained ZnO is confirmed with values obtained from XRD calculations.

3.3. Optical absorption studies.

Optical absorption spectrum of RGO, ZnO, and RGO/ZnO nanocomposites samples were measured by UV-Vis spectrophotometer in the range 200-900 nm as shown in Fig. 5. (a, b, c). The figure depicted that for RGO there are main absorption peak at 246 nm and another shoulder peak at 299 nm which refer to respectively to (C-C) and (C=C) bonds between the carbon atoms of reduced graphene oxide. In zinc oxide the main peak exists at 276 nm, but in RGO/ZnO nanocomposites in different ratios from RGO/ZnO1 to RGO/ZnO5 the exciton peak moved from 364 nm to 374 nm which mean that zinc oxide nanoparticles are stacked well on RGO nanosheets and the displacement in the peak is due to the difference in ZnO ratio which agree with the images obtained by TEM.

The corresponding excitonic energy (E_{ex}) was calculated from the following formula.

$E_{ex} = hC/\lambda_{max}$ (11)

Where h is Planck's constant, C is the velocity of light, and λ_{max} is the exciton peak wavelength.It is shown that increasing ZnO ratio leads to a red shift in both of the exciton peaks. The optical absorption spectra were analyzed according to Tauc`s relation in the form:

$$\alpha h\nu = B(\alpha h\nu - E_g)^r \quad (12)$$

Where α is absorption, hν is the photon energy , E_g is the optical band gap and B is the steepness or ordering parameter. The Tauc's relation for direct band gap [24]:

$(Ah\nu)^2 = B\,(h\nu - E_g)^r$ (13)

Where *B* is the edge width parameter representing the film quality, E_g is the optical energy gap of the material, which refer to the direct band gap of optical transitions. Fig.5. (d) describes the change in Exiton peak with ZnO mass ratio and it's obviously show that Eg increasing with the increasing in graphene ratio and this because the Eg of graphene is higher than Eg of ZnO . It is observed that the values of E_g decreases with increasing ZnO ratio as shown in table (3). The noticeable reduction in E_g and E_{ex} may be ascribed to the increase in the crystallite size due to the improvement in crystallinity by ZnO incorporation in graphene matrix also became E_g for ZnO is lower than E_g for RGO..

The absorption coefficients near the fundamental absorption edge are exponentially dependent on the photon energy, and obey Urbach's empirical relation [25].

$$\alpha = \alpha_0 exp\left(\frac{h\nu}{E_e}\right) \quad (14)$$

$$\text{Ln } \alpha = \alpha_0 + \left(\frac{h\nu}{E_e}\right) \quad (15)$$

Where α_0 is a constant and E_e is Urbach energy which is interpreted as the width of band tail of localized states in the band gap and in general represents the degree of disorder in an amorphous semiconductor, the absorption in this region is due to transitions between extended states in one band and localized states in the exponential tail of the other band.

The photon energy dependence of the absorption coefficient can be described by Urbach's relation given by Eq. (14, 15). Fig. 6. (a) shows a plot of ln(α) versus hν of pure RGO and pure ZnO, Fig. 6. (b) shows a plot of ln(α) versus hν of RGO/ZnO nanocomposites. that should give a linear

portion with a slope equal to the inverse of E_e and the obtained E_e values are given in Table 3. The E_e values of the RGO/ZnO are increased with increasing ZnO content. One noted that the values of E_e are changed inversely with those of E_g and this may be due to the increase of the disorder of RGO matrix by ZnO doping. This increase leads to are distribution of states from band to tail and thus allows for a large number of possible bands to tail and tail to tail transitions.

Table (3) Exiton peak and energy gap (E_g) for pure ZnO, pure RGO and RGO/ZnO nanocomposites

Sample	Exiton peak (nm)	Energy gap (E_g)
ZnO	376	3.34
RGO	268	2.39
RGO/ZnO 1	361	2.51
RGO/ZnO 2	365	2.87
RGO/ZnO 3	368	3.08
RGO/ZnO 4	371	3.27
RGO/ZnO 5	372	3.3

Figure 7. (a) shows the energy gap determination of pure RGO, Fig. 7. (b) shows Energy gap determination of pure ZnO and Fig. 7. (c) shows the effect of ZnO ratio on energy gap value. Energy gap of ZnO is 3.34 eV, 2.39 eV for reduced graphene oxide, and it's clear that energy gap is gradually increased with the increasing of ZnO continent in composites may be energy gap in RGO is more than energy gap in ZnO or the increasing in grain size of nanocomposite with increasing in ZnO mass ratio.

The effect of UV irradiation on the absorbance and other optical properties was studied by putting diluted solution sample under UV lamp and measure the absorbance every half hour as shown in Fig. 8. It can be seen that increasing UV irradiation dose results in enhancement in the absorption according by blue shift in E_g values due to induced UV effect.

3.4. FT – IR Spectroscopy

Fourier transforms infrared spectroscopy (FT-IR) is obtained as transmission spectra of KBr sample pellets in order to characterize the bond of structure of RGO, ZnO, and RGO/ZnO nanocomposites. Figure 9. (a, b, c) shows (FT-IR) of RGO, ZnO, and RGO/ZnO nanocomposites in the range of 4000 to 400 cm^{-1}. The absorbance peak of reduced graphene oxide at the high frequencies contend at 3457 cm^{-1} refers to a large amount hydroxyl group (O-H) which refer to the moisture in sample this may be from KBr or the sample contain some water remain after drying and also 2341 cm^{-1}, wide spectra transmittance peak from 2000 cm^{-1} to 3500 cm^{-1} corresponding to the absorption of water molecule and that indicate the high of moisture of RGO. The transmittance peak at 1122 cm^{-1} represent the (C-O) bonds and (C-OH) on the surface of RGO nanosheets. At the other side in zinc oxide the absorption peak at high frequencies area also refer to the moisture of water molecule such as at 3435 cm^{-1} and peak at 562 cm^{-1} represent the (Zn-O) bonds as shown in table 4. Figure 9. (c) show that with increasing in ZnO mass ratio in samples (Zn-O) bond peak is stretched and shifted to left.

Table (4) FT-IR peaks and their characteristic bonds for ZnO

FT-IR peak (cm^{-1})	**3435**	**2993**	**2861**	**2359**	**1635**	**1401**	**1122**
Bond	O-H	C-H	C-H	CO_2	C=C	C=O	C-O

4. CONCLUSION

In summery reduced grapheme oxide (RGO) were synthesized via modified Hummer's method at low temperature process and RGO/ZnO nanocomposites were synthesized via facile low temperature hydrothermal method. It obviously from TEM images that ZnO nanoparticles are homogeneously decorated on the surface of RGO sheets and stack on RGO sheets. FT-IR spectra ensure the formation of nanocomposites. This facile synthesis method can be easily used to the synthesis of other RGO-based hybrid nanocomposite materials for many purposes such as electrochemical based sensors or photodegradation.

REFERENCES

[1] Y. Zhang, Z. Kang, X. Yan, and Q. Liao, “ZnO nanostructures in enzyme

biosensors," *Sci. China Mater.*, vol. 58, no. 1, pp. 60–76, 2015.

[2] W. S. Hummers Jr and R. E. Offeman, "Preparation of graphitic oxide," *J. Am. Chem. Soc.*, vol. 80, no. 6, p. 1339, 1958.

[3] K. Anand, O. Singh, M. P. Singh, J. Kaur, and R. C. Singh, "Hydrogen sensor based on graphene/ZnO nanocomposite," *Sensors Actuators B Chem.*, vol. 195, pp. 409–415, 2014.

[4] K. Subramani and M. Sathish, "Facile synthesis of ZnO nanoflowers/reduced graphene oxide nanocomposite using zinc hexacyanoferrate for supercapacitor applications," *Mater. Lett.*, vol. 236, pp. 424–427, 2019.

[5] M. Pumera, "Graphene in biosensing," *Mater. today*, vol. 14, no. 7–8, pp. 308–315, 2011.

[6] J. W. Park, C. Lee, and J. Jang, "High-performance field-effect transistor-type glucose biosensor based on nanohybrids of carboxylated polypyrrole nanotube wrapped graphene sheet transducer," *Sensors Actuators B Chem.*, vol. 208, pp. 532–537, 2015.

[7] Q. Xiang, J. Yu, and M. Jaroniec, "Graphene-based semiconductor photocatalysts," *Chem. Soc. Rev.*, vol. 41, no. 2, pp. 782–796, 2012.

[8] K. I. Bolotin *et al.*, "Ultrahigh electron mobility in suspended graphene," *Solid State Commun.*, vol. 146, no. 9–10, pp. 351–355, 2008.

[9] G. Ning, Z. Fan, G. Wang, J. Gao, W. Qian, and F. Wei, "Gram-scale synthesis of nanomesh graphene with high surface area and its application in supercapacitor electrodes," *Chem. Commun.*, vol. 47, no. 21, pp. 5976–5978, 2011.

[10] S. Stankovich *et al.*, "Synthesis of graphene-based nanosheets via chemical reduction of exfoliated graphite oxide," *Carbon N. Y.*, vol. 45, no. 7, pp. 1558–1565, 2007.

[11] Y.-M. Lin and P. Avouris, "Strong suppression of electrical noise in bilayer graphene nanodevices," *Nano Lett.*, vol. 8, no. 8, pp. 2119–2125, 2008.

[12] M. Azarang, A. Shuhaimi, R. Yousefi, A. M. Golsheikh, and M. Sookhakian, "Synthesis and characterization of ZnO NPs/reduced graphene oxide nanocomposite prepared in gelatin medium as highly efficient photo-degradation of MB," *Ceram. Int.*, vol. 40, no. 7, pp. 10217–10221, 2014.

[13] S. H. Song *et al.*, "Highly Efficient Light-Emitting Diode of Graphene Quantum Dots Fabricated from Graphite Intercalation Compounds," *Adv. Opt. Mater.*, vol. 2, no. 11, pp. 1016–1023, 2014.

[14] E. R. Ezeigwe, M. T. T. Tan, P. S. Khiew, and C. W. Siong, "One-step green

synthesis of graphene/ZnO nanocomposites for electrochemical capacitors," *Ceram. Int.*, vol. 41, no. 1, pp. 715–724, 2015.

[15] S. S. Low, M. T. T. Tan, H.-S. Loh, P. S. Khiew, and W. S. Chiu, "Facile hydrothermal growth graphene/ZnO nanocomposite for development of enhanced biosensor," *Anal. Chim. Acta*, vol. 903, pp. 131–141, 2016.

[16] J. S. Y. Chia *et al.*, "A novel one step synthesis of graphene via sonochemical-assisted solvent exfoliation approach for electrochemical sensing application," *Chem. Eng. J.*, vol. 249, pp. 270–278, 2014.

[17] Y. Li, D. Wang, W. Li, and Y. He, "Photoelectric conversion properties of electrochemically codeposited graphene oxide–ZnO nanocomposite films," *J. Alloys Compd.*, vol. 648, pp. 942–950, 2015.

[18] S. S. P. Haghshenas, A. Nemati, R. Simchi, and C.-U. Kim, "Photocatalytic and photoluminescence properties of ZnO/graphene quasi core-shell nanoparticles," *Ceram. Int.*, vol. 45, no. 7, pp. 8945–8961, 2019.

[19] J. Ding *et al.*, "Hydrothermal synthesis of zinc oxide-reduced graphene oxide nanocomposites for an electrochemical hydrazine sensor," *RSC Adv.*, vol. 5, no. 29, pp. 22935–22942, 2015.

[20] M. N. Conde *et al.*, "Preparation of ZnO nanoparticles without any annealing and ripening treatment," *J. Mater. Sci. Eng. A*, vol. 1, no. 7A, p. 985, 2011.

[21] P. Scherrer, "Göttinger Nachrichten Math," *Phys*, vol. 2, pp. 98–100, 1918.

[22] G. K. Williamson and W. H. Hall, "X-ray line broadening from filed aluminium and wolfram," *Acta Metall.*, vol. 1, no. 1, pp. 22–31, 1953.

[23] S. Kumar, P. Sharma, and V. Sharma, "CdS nanofilms: synthesis and the role of annealing on structural and optical properties," *J. Appl. Phys.*, vol. 111, no. 4, p. 43519, 2012.

[24] J. Tauc and A. Menth, "States in the gap," *J. Non. Cryst. Solids*, vol. 8, pp. 569–585, 1972.

[25] M. V Kurik, "Urbach rule," *Phys. status solidi*, vol. 8, no. 1, pp. 9–45, 1971.

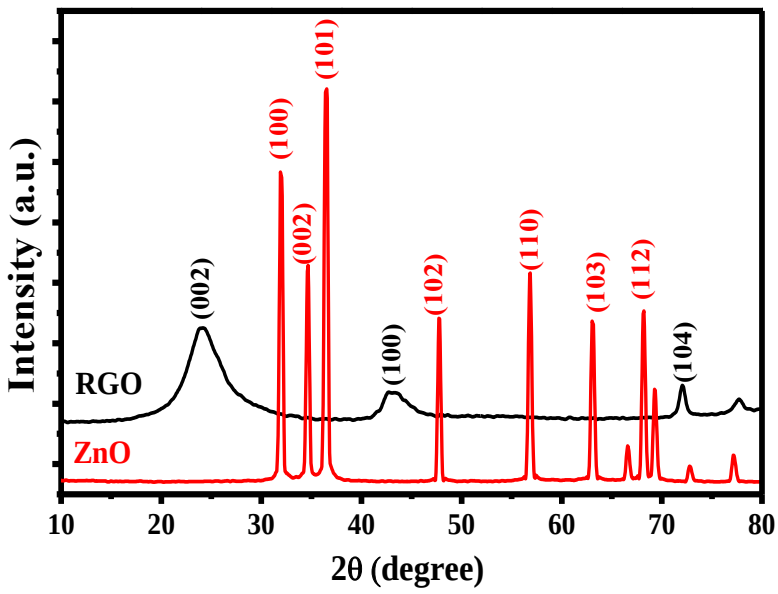

Fig. 1. (a). XRD patterns for pure reduced graphene oxide and pure zinc oxide.

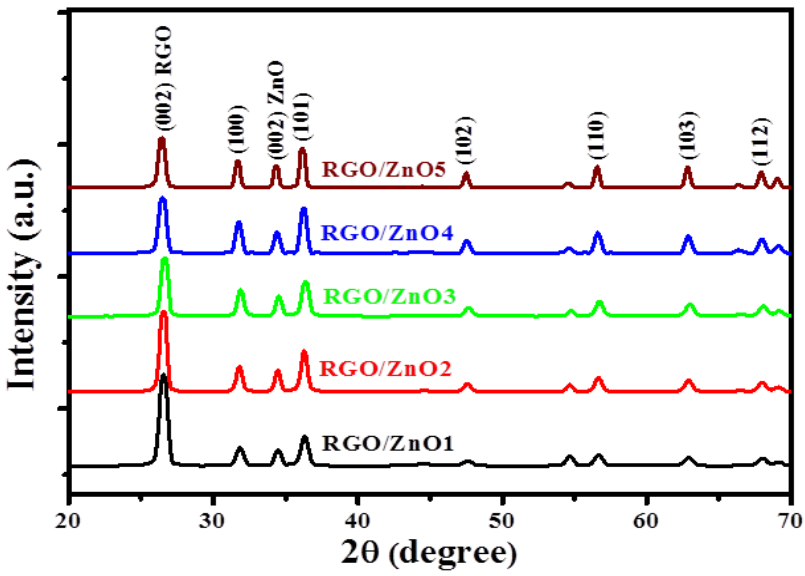

Fig. 1. (b) XRD patterns for RGO/ZnO nanocomposites.

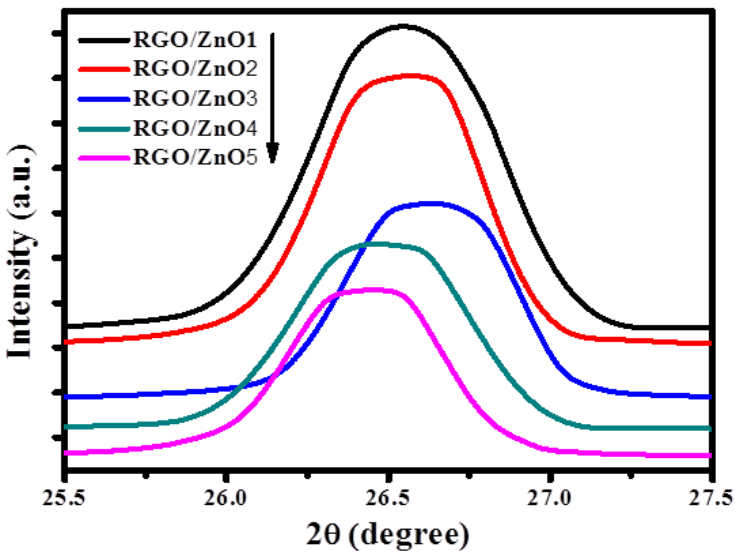

Fig. 2 (a). The diffraction peak shift against 2θ of (002) crystalline plane of RGO/ZnO nanocomposites.

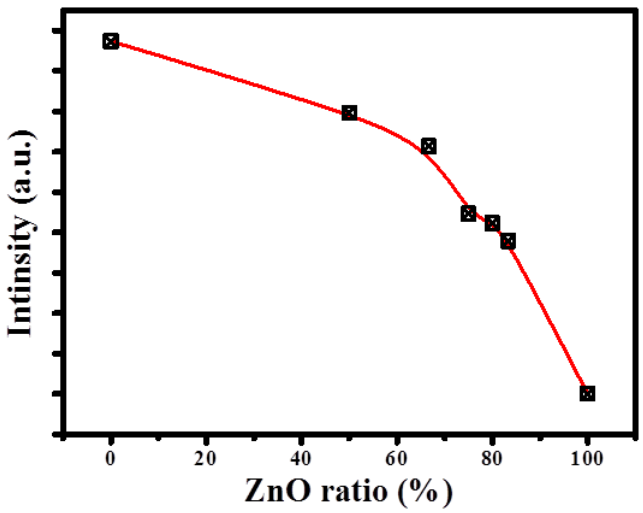

Fig. 2. : The peak shift of (002) crystalline plane of RGO/ZnO nanocomposites.

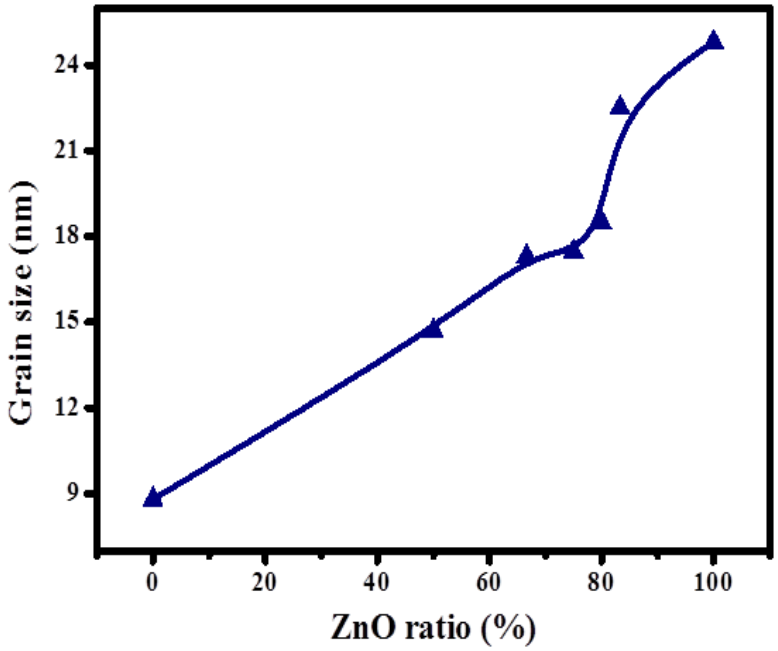

Fig. 3. The dependence of the grain size with ZnO ratio

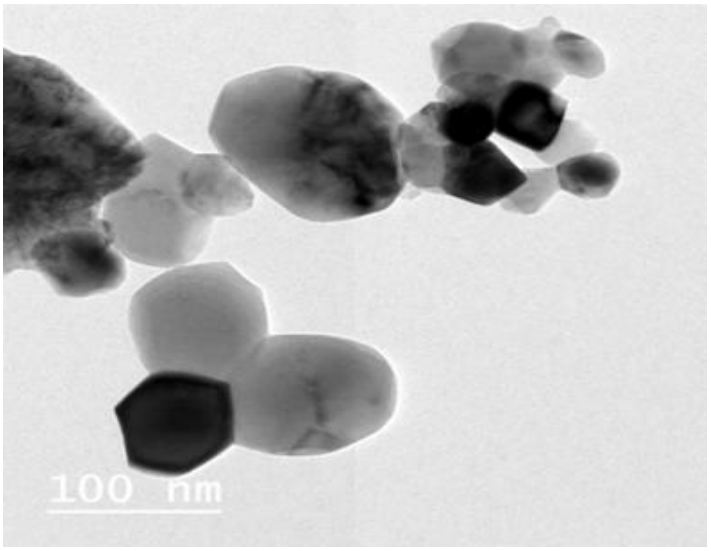

Fig.4. (a). HRTEM Image of pure Zinc Oxide (ZnO) nanopowder.

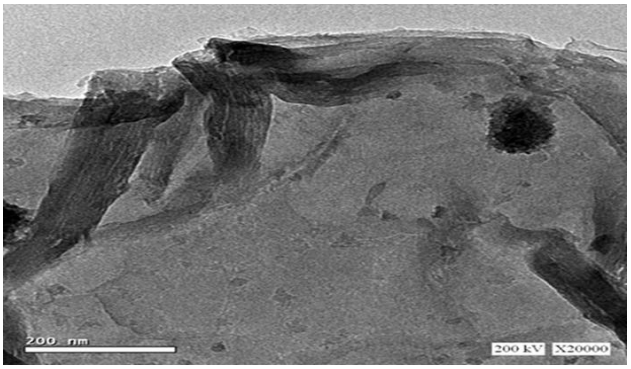

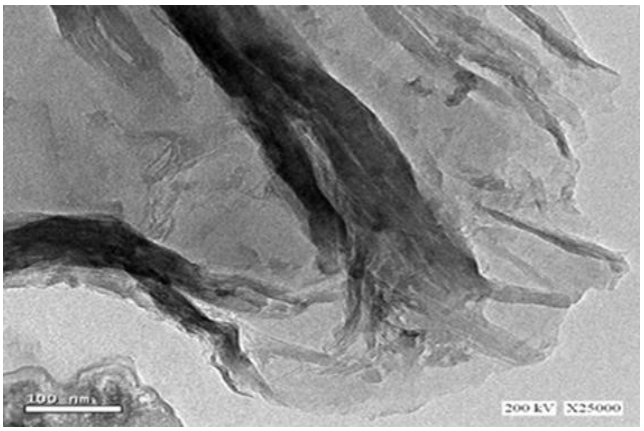

Fig. 4. (b). HRTEM images of reduced grapheme oxide (RGO) nanopowder.

Fig. 4. (c). HRTEM Image RGO/ZnO nanocomposites.

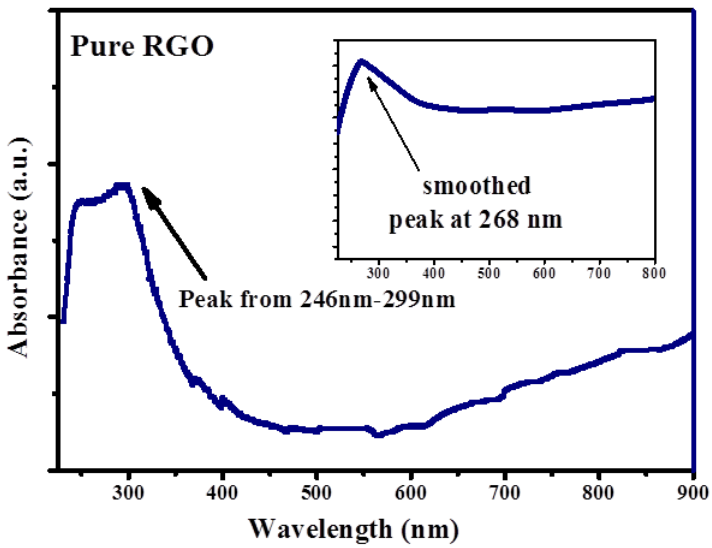

Fig. 5. (a) Absorption versus the incident wavelength for RGO. The inset shown the smoothed peak at 268nm

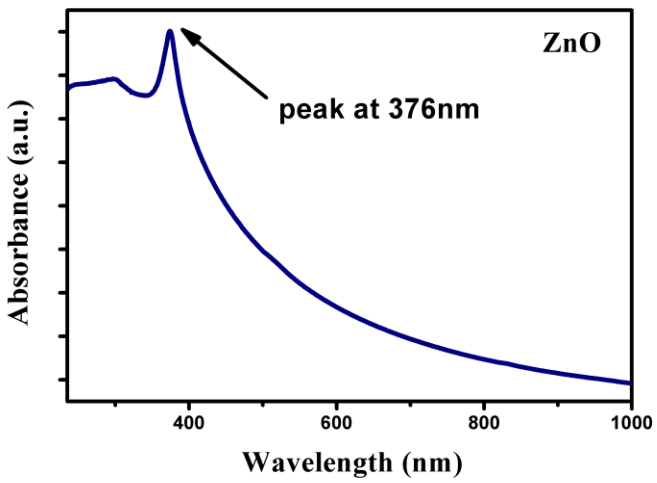

Fig. 5. (b) Absorbance versus wavelength for pure ZnO.

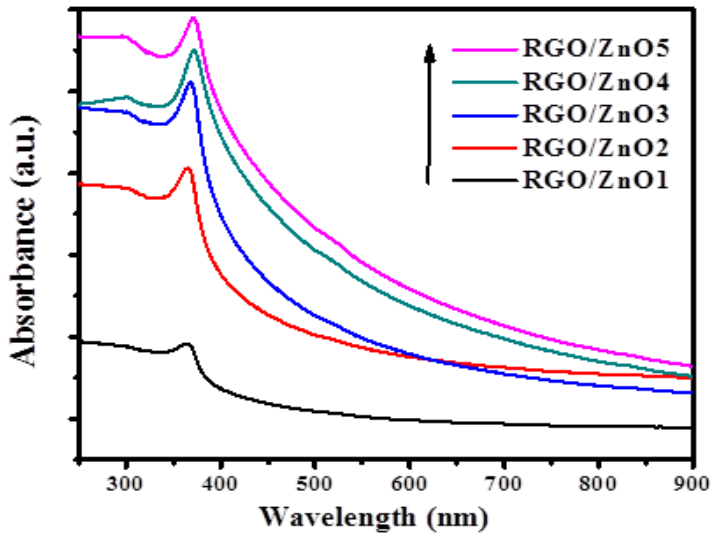

Fig. 5. (c) Absorbance versus the incident wavelength for RGO/ZnO nanocomposites.

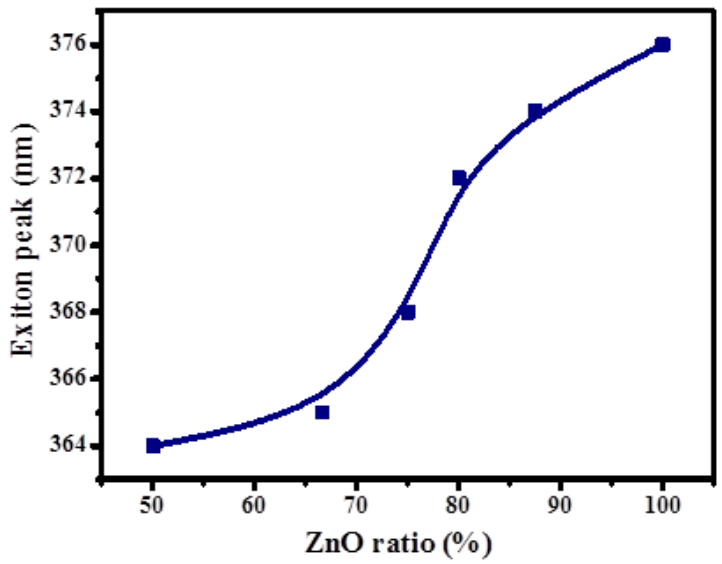

Fig. 5. (d) The dependence of the exciton peak energy on ZnO ratio for RGO/ZnO nanocomposites.

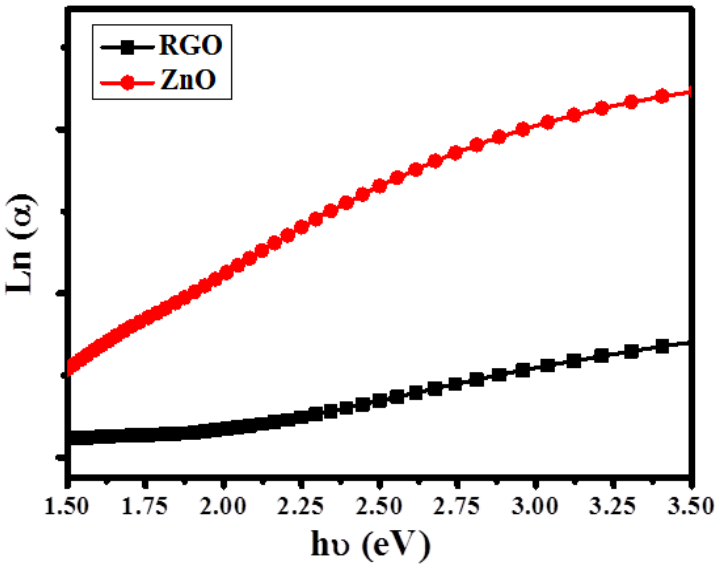

Fig. 6. (a). Plot of Ln(α) versus h**ν** of pure RGO and pure ZnO.

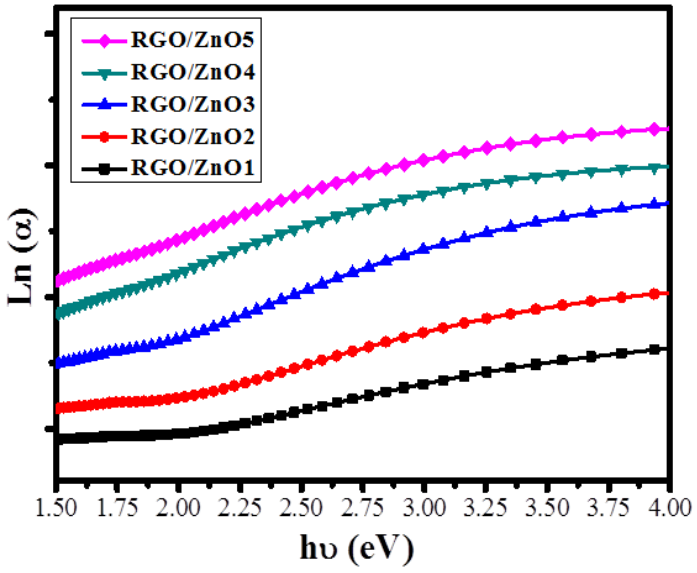

Fig. 6. (b) lnα versus hν for RGO/ZnO nanocomposites.

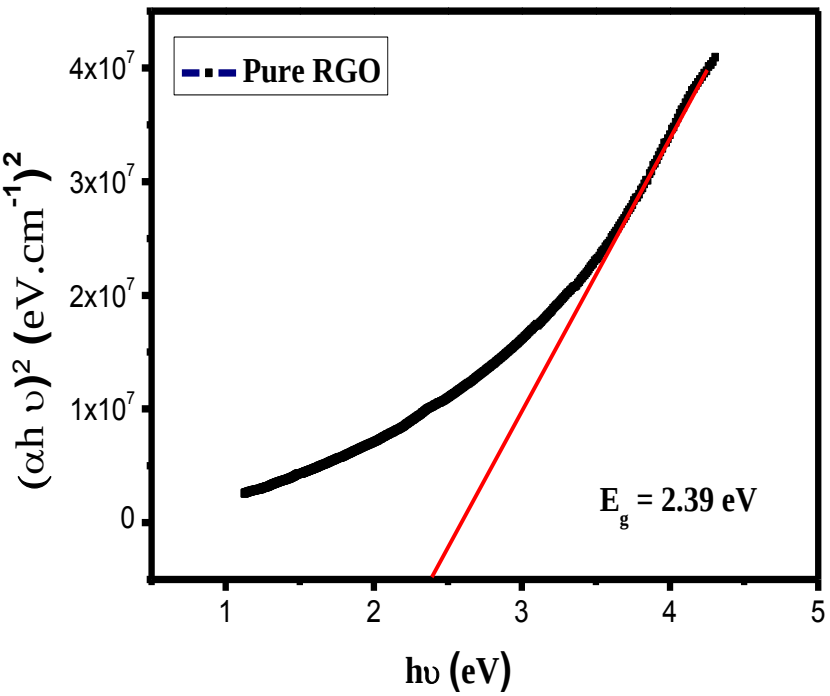

Fig. 7. (a) Energy gap determination of pure RGO.

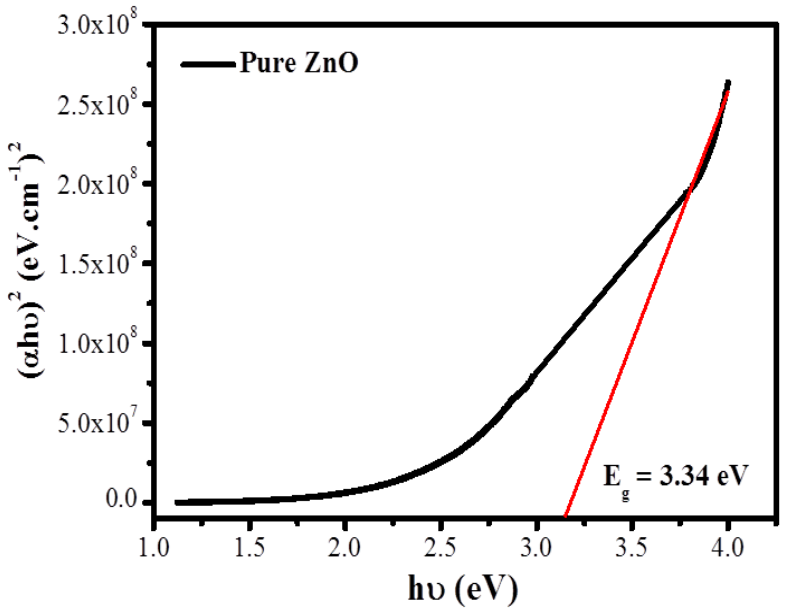

Fig. 7. (b) Energy gap determination of pure ZnO.

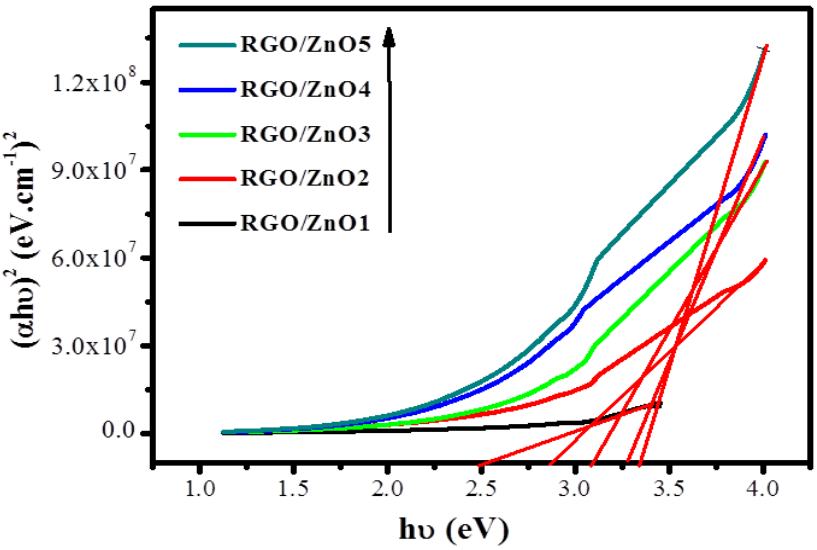

Fig. 7. (c) Energy gap determination of RGO/ZnO nanocomposites.

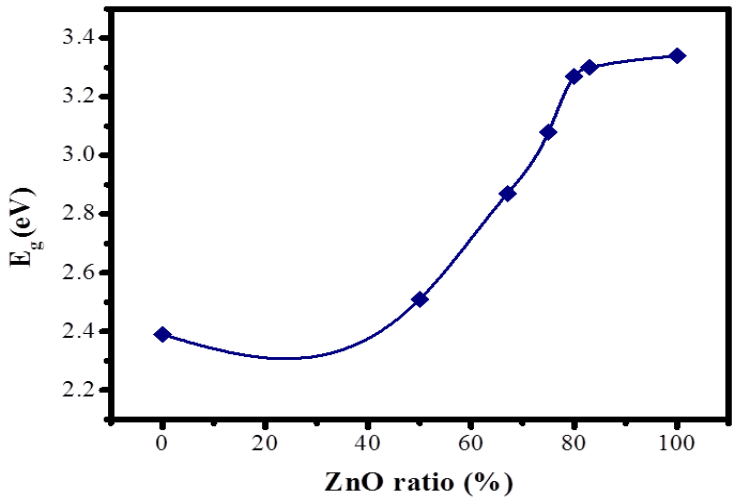

Fig. 7. (d) The dependence of energy gap on ZnO ratio for RGO/ZnO nanocomposites.

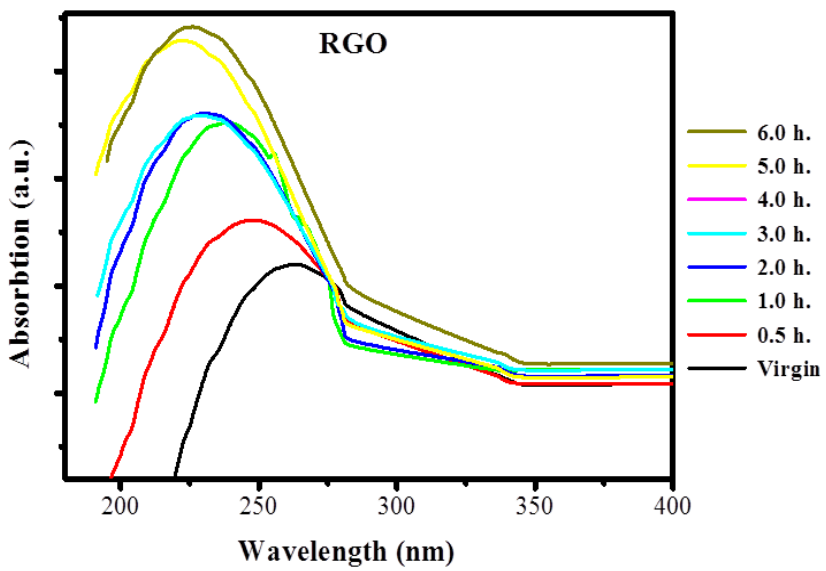

Fig. 8. (a) Effect of UV irradiation dose on the absorbance spectra of RGO.

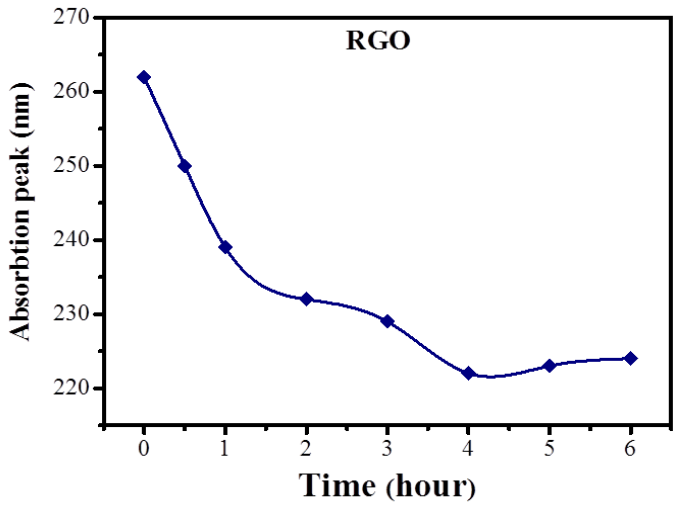

Fig. 8. (b) Effect of UV irradiation dose on the absorbance peak shift of pure RGO.

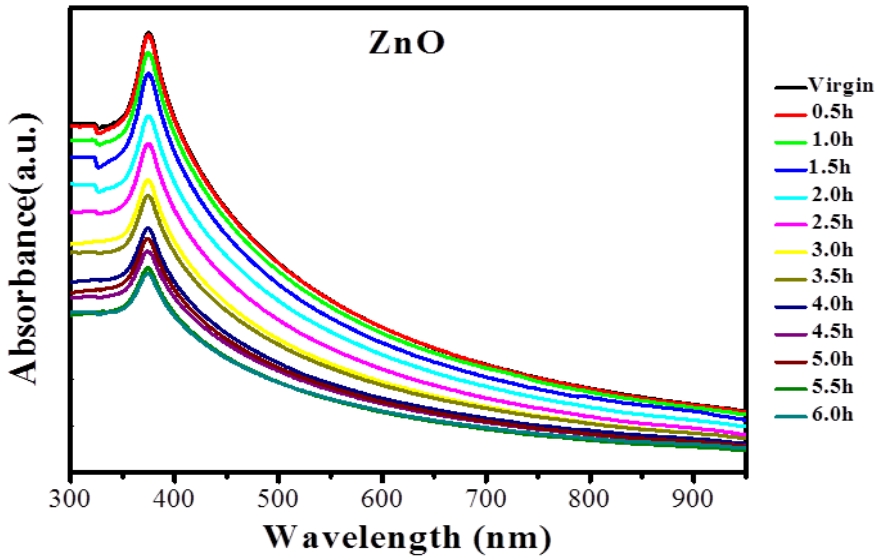

Fig. 8. (c) Effect of UV irradiation dose on the absorption spectra of pure ZnO.

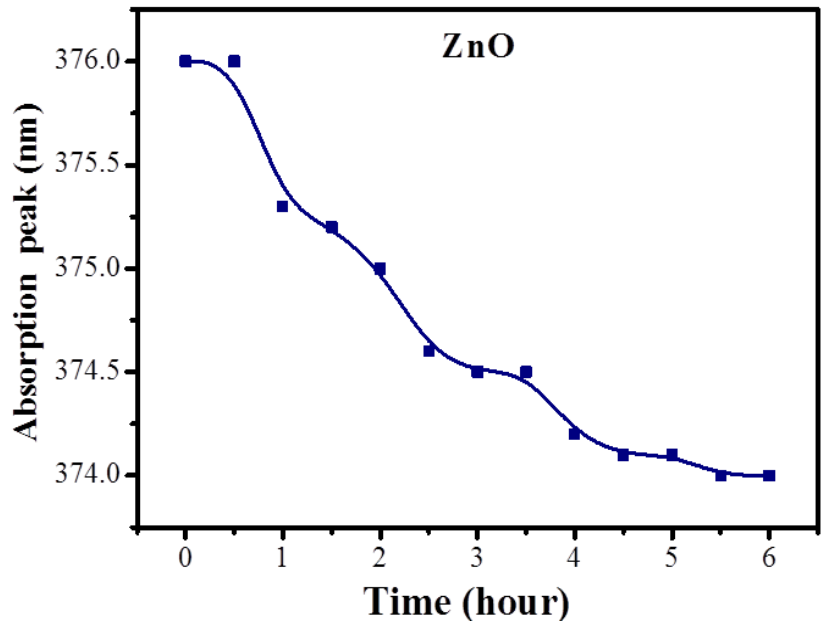

Fig. 8. (d) Effect of UV irradiation dose on the peak shift of pure ZnO.

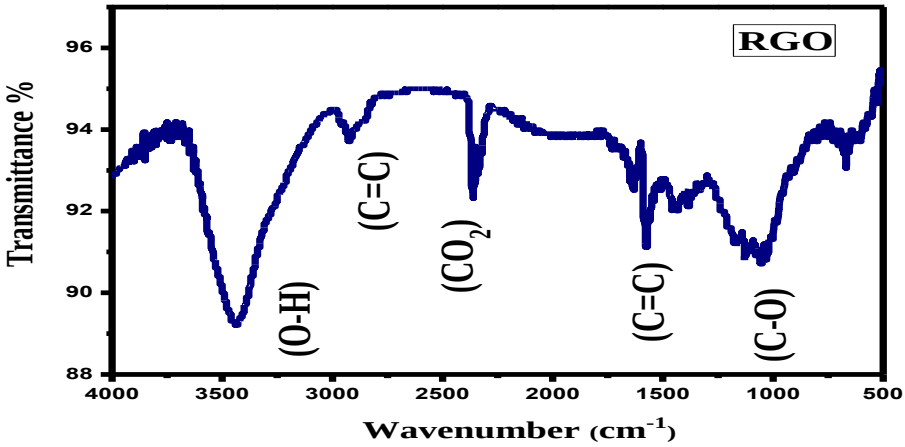

Fig.9. (a). FT-IR spectra of reduced graphene oxide (RGO).

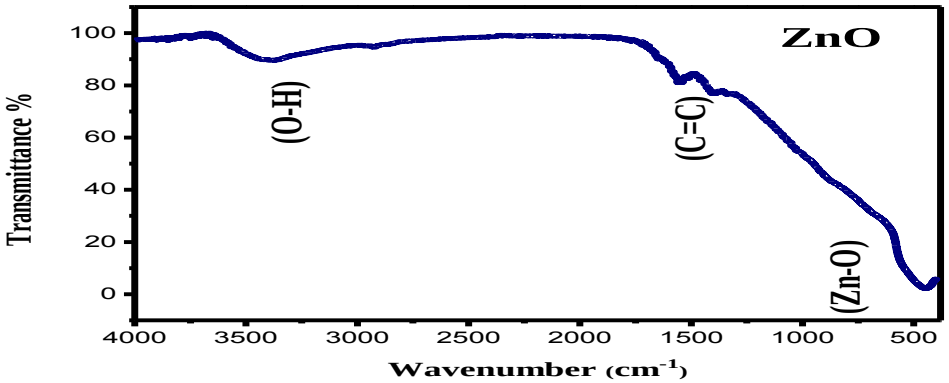

Fig. 9. (b) FT-IR spectra of pure ZnO.

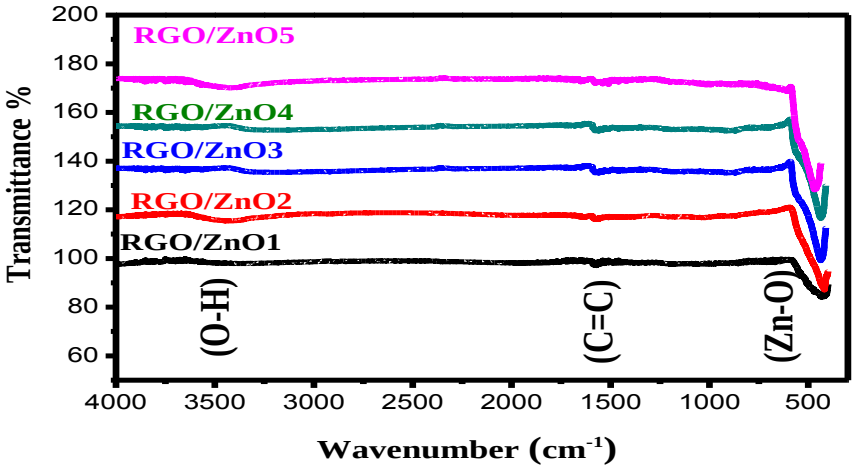

Fig. 9. (c). FT-IR spectra of RGO/ZnO nanocomposites.